ELSEVIER

Biochemical Pharmacology 64 (2002) 1215–1226

Biochemical Pharmacology

Contribution of apoptosis in the cytotoxicity of the oxaliplatin–irinotecan combination in the HT29 human colon adenocarcinoma cell line

Stéphanie Arnould[a,b], Sylvie Guichard[a,b], Isabelle Hennebelle[a], Georges Cassar[c], Roland Bugat[a,b], Pierre Canal[a,*]

[a]*Groupe de Pharmacologie Clinique et Expérimentale, Institut Claudius Regaud, EA 3035, 20-24 rue du Pont Saint Pierre, 31052 Toulouse Cedex, France*

[b]*Université Paul Sabatier, 118 route de Narbonne, 31062 Toulouse Cedex, France*

[c]*INSERM U395, Service Commun d'Analyse et de Tri Cellulaires, IFR30 Centre Hospitalier Universitaire Purpan, Toulouse Cedex, France*

Received 31 December 2001; accepted 26 June 2002

Abstract

Interactions between the topoisomerase I inhibitor irinotecan (CPT-11) and the platinum derivative oxaliplatin (L-OHP) were investigated in HT29 colon cancer cell line. Synergism was observed when cells were simultaneously exposed to drugs or when cells were first exposed to CPT-11. Flow cytometric studies showed a G_2/M accumulation when cells were exposed to the simultaneous and CPT-11 → L-OHP combinations whereas a persistent S phase delay was observed when cells were first exposed to L-OHP. We characterised the cytotoxic effect by assessing the induction of apoptosis. Irinotecan induced substantial DEVDase activity and poly(ADP-ribose) polymerase cleavage while this activity was moderate and delayed after exposure to L-OHP. Combination experiments showed a sequence-dependent onset of apoptosis, the CPT-11 → L-OHP schedule being the earliest and the most effective; on the other hand the apoptotic signaling generated by CPT-11 was partly inhibited in the simultaneous combination and in the L-OHP → CPT-11 sequence. Cell death studies using a dual staining technique showed a shift from apoptosis to necrosis when combining these drugs at high concentrations. Synergistic interactions observed using CPT-11 before L-OHP may be linked to an early apoptotic signaling while the L-OHP-induced S phase block could account for the observed additive effect in the reverse sequence. An additional phenomenon might work towards synergism for the simultaneous combination.

Keywords: Oxaliplatin; Irinotecan; Synergism; Apoptosis; Poly(ADP-ribose) polymerase; Cell cycle

1. Introduction

The camptothecin derivative irinotecan (CPT-11) is a prodrug of the most potent topoisomerase I (Topo I) inhibitor SN-38. Topoisomerase I is a nuclear enzyme which modifies DNA topology by producing transient single strand breaks thereby decreasing constraints due to supercoiling during replication, transcription, repair and recombination processes [1]. Topoisomerase I inhibitors exert their cytotoxic effect by stabilising DNA–Topo I cleavable complexes [2] and inhibiting DNA religation step. Collision between these complexes and replication forks induces lethal double-strand breaks [3]. Irinotecan is active in many tumour models [4,5] and is the first chemotherapeutic drug displaying clinical efficacy in the treatment of advanced colorectal cancer in chemotherapy-naive or 5-fluorouracil-pre-treated patients since the introduction of 5-FU [6,7]. Irinotecan is therefore an effective second-line chemotherapy in colorectal cancer. It has also been tested in combination with the LV5FU2 reference regimen [8], or with anticancer agents such as mitomycin C [9] and L-OHP [10]. L-OHP is a third-generation platinum derivative bearing a 1,2-diaminocyclohexane (DACH) carrier ligand. Cytotoxicity of platinum derivatives is characterised by formation of platinum adducts on DNA among which Pt-GG and Pt-AG intrastrand crosslinks are the major lesions [11]. L-OHP showed a broad *in vitro* activity [12] and was particularly effective in CDDP-resistant cells, notably colon cancer cell lines which suggests that L-OHP might have cellular targets,

* Corresponding author. Tel.: +33-5-61-42-42-22; fax: +33-5-61-42-41-77.

E-mail address: canal@icr.fnclcc.fr (P. Canal).

Abbreviations: CPT-11, irinotecan; L-OHP, oxaliplatin; PARP, poly-(ADP-ribose) polymerase; PI, propidium iodide; Ho342, Hoechst 33342; CDDP, cisplatin; DNA-PK, DNA-dependent protein kinase.

0006-2952/02/$ – see front matter
PII: S0006-2952(02)01291-1

mechanisms of action and/or mechanisms of resistance different from CDDP [13]. Phase II studies report a moderate L-OHP activity as second-line treatment in colorectal cancers; this distinguishes this drug from CDDP and carboplatin for which no objective response had ever been reported in this indication [14]. Combination of L-OHP with 5-FU and folinic acid confirms a therapeutic benefit compared to this standard regimen in naive or pre-treated patients [15,16]. Irinotecan and L-OHP having different mechanisms of action, broad spectra of cytotoxic and antitumour activity and displaying no cross-resistance provided a rationale for the *in vitro* and *in vivo* study of their combination. In clinical practice, their association resulted in an increase in the objective response rate [17,18].

Apoptosis is a physiological process by which multicellular organisms eliminate cells in order to maintain homeostasis. This genetically regulated mechanism occurs during embryonic development, maturation of the immune system but also in many pathological situations [19,20]. Many chemotherapeutic drugs among which topoisomerase I and II inhibitors induce programmed cell death in different cell lines [21], but no data is available in colon cancer cell lines exposed to L-OHP.

The aim of this study was to characterise the cytotoxic effect and to determine interactions between L-OHP and CPT-11 in the HT29 colon adenocarcinoma cell line. We first evaluated their cytotoxicity using three different combination schedules and focused our interest on their effects on the cell cycle. We then assessed the induction of cell death, namely apoptosis, by studying PARP cleavage, quantitating DEVDase activity and performing double-parameter flow cytometry following the same schedules as tested for cytotoxicity studies.

2. Materials and methods

2.1. Drugs and chemicals

Rhône-Poulenc Rorer and Sanofi Winthrop laboratories provided CPT-11 and L-OHP, respectively. RPMI 1640 was purchased from Eurobio and foetal calf serum was from Biochrom KG. Sulforhodamine B and trichloroacetic acid were purchased from Sigma Chemical Co. Polyclonal rabbit anti-PARP and mouse monoclonal anti-actin antibodies were purchased from Roche Molecular Biochemicals. Anti-rabbit and anti-mouse horseradish peroxydase-conjugated antibodies were purchased from Amersham Pharmacia Biotech and Bio-Rad, respectively.

2.2. Cell culture

HT29 colon cancer cell line was from American Type Culture Collection. Cells were grown as monolayers in RPMI 1640 medium supplemented with 5% foetal calf serum and 2 mM L-glutamine at 37° in a humidified atmosphere containing 5% CO_2. Cells were trypsinised once a week with trypsin/EDTA (0.25%/0.02%) (Eurobio) and medium was changed once a week. Cells were grown without antibiotics and were regularly tested for mycoplasma contamination. Doubling time was 28 hr.

2.3. Cytotoxicity studies

Cytotoxicity studies were performed using the sulforhodamine B technique [22] representing the percentage of cell growth compared to a control after exposure to increasing drug concentrations. Cytotoxicity of each drug was evaluated by the IC_{50} value. On day 1, 2200 cells were plated in 96-well plates in a volume of 150 μL per well. In each plate, one column contained cells not exposed to the drugs while nine columns contained cells exposed to increasing concentrations of L-OHP or CPT-11. Six wells were used for each concentration. On day 2 or days 2 and 3, L-OHP and CPT-11 were added in a volume of 50 μL resulting in a series of final concentrations ranging from 0.05 to 100 μM for L-OHP and 0.25 to 100 μM for CPT-11. For combination studies, concentrations were 5-fold reduced with a L-OHP:CPT-11 ratio of 1:4 (molar ratio of IC_{50} values) and three different schedules of exposure were tested: L-OHP for 24 hr then CPT-11 for 24 hr; CPT-11 for 24 hr then L-OHP for 24 hr; L-OHP and CPT-11 simultaneously for 24 hr. After drug exposure, the medium in control and drug-containing wells was removed, cells were washed with cold PBS and 200 μL of fresh drug-free medium were added to each well. Cells were cultured for three doubling times after the end of drug exposure and were then precipitated with ice-cold 50% trichloroacetic acid and fixed for 60 min at 4°, washed five times with tap water and air-dried. Fixed cells were then dyed with 50 μL of 0.4% sulforhodamine B in 1% acetic acid solution, washed with 1% acetic acid and air-dried. Sulforhodamine B was dissolved in 150 μL of 10 mM Tris buffer pH 10.5 and 540 nm optical density was measured in a Labsystems Multiskan® Multisoft apparatus. Each experiment was performed three times.

2.4. Median-effect analysis

Median-effect analysis was performed using the method described by Chou and Talalay [23]. The type of interaction between L-OHP and CPT-11 was evaluated by comparing the cytotoxic effects obtained after sequential or simultaneous exposures to the drugs with the ones observed after exposure to L-OHP or CPT-11 alone. The median-effect analysis was performed by ensuring that all the recommended requirements were met, i.e. (a) every median-effect plot had a correlation coefficient for the regression lines greater than 0.95; (b) the slopes of the dose–effect curves were always superior to 1 in order to obtain the best sigmoïdicity and (c) the median-effect doses (Dm) were consistent with the IC_{50} values that were graphically obtained. Interactions were calculated as

mutually non-exclusive case combination index (CI) for each fraction affected. A CI value < 1 indicates synergism, $CI = 1$ indicates additivity and $CI > 1$ characterises an antagonistic interaction.

2.5. Drug exposure

Exponentially growing cells were exposed to either 1.23 μM L-OHP for 24 hr or 4.6 μM CPT-11 for 24 hr or combinations of the two drugs which corresponded to IC_{50}. Higher drug concentrations were used to emphasise specific effects, i.e. 5 μM L-OHP for 24 hr or 20 μM CPT-11 for 24 hr or combinations of the two drugs. Medium was then removed and replaced with a drug-free one. Cells were harvested at the end of the exposure and 24, 48, 72 or 96 hr afterwards.

2.6. Flow cytometric analysis of cell cycle phase distribution

Exponentially growing cells (10^7) were exposed to L-OHP, CPT-11 or their combinations according to the aforementioned schedules. Adherent cells were washed once with ice-cold PBS, trypsinised and counted. One million cells per sample were fixed in ice-cold 70% ethanol and stored at −20° until analysis. Cells were then washed in PBS before being suspended in 1 mL staining solution (20 μg/mL PI (Sigma), 0.1% Triton X-100 (Sigma), 200 μg/mL ribonuclease A (Sigma) in PBS) and incubated at 37° for 15 min. Analysis of 10,000 events was performed on a FACScan flow cytometer (Becton Dickinson). DNA fluorescence was collected in linear mode using a doublet discrimination gate and cell cycle distribution was quantitated using CellFit software. Each experiment was performed three times.

2.7. Detection of PARP cleavage by Western blot analysis

Cell pellets (one million cells were seeded per dish) were sonicated three times for 5 s in a lysis buffer (62.5 mM Tris, 4 M urea, 10% glycerol, 2% SDS, 0.04% bromophenol blue, 100 mM dithiothreitol) and protein concentration was determined using the method described by Bradford [24]. Proteins (20 μg) were boiled in a water bath at 95° for 5 min, separated by SDS–PAGE consisting of a 4% (w/v) acrylamide stacking gel and a 7.5% (w/v) acrylamide resolving gel containing 0.1% SDS and electrotransferred onto a polyvinylidene fluoride membrane (Amersham Pharmacia Biotech). Membranes were blocked with 5% non-fat dry milk in TBS 0.1% Tween 20 and incubated overnight at 4° with either anti-PARP (1/10,000) or anti-actin (1/25,000) antibody. Membranes were then exposed to secondary antibodies (1/5000) for 90 min. Immune complexes were detected by the ECL plus system (Amersham Pharmacia Biotech) and Western blots were scanned with a Molecular Dynamics Storm 840 optical scanner. The intensity of each band was determined using Image Quant 1.0 software. The percentage of cleaved PARP was determined according to the method described by He *et al.* [25]:

$$\text{PARP cleavage}\,(\%) = \left[\frac{\text{intensity of } M_r\,85,000 \text{ band}}{\text{intensity of } M_r\,85,000 \text{ band} + \text{intensity of } M_r\,116,000 \text{ band}}\right] \times 100$$

Each experiment was performed three times.

2.8. Determination of DEVDase activity

DEVDase activity was assayed using the Caspase-3/CPP32 colorimetric kit (Biosource International). Cell pellets were suspended in the lysis buffer provided by the manufacturer and protein concentration was assayed as previously described. Cytosolic proteins (100 μg) were incubated at 37° for 2 hr with 200 μM DEVD–*p*NA substrate and product formation was measured at an emission wavelength of 405 nm using a Labsystems Multiskan® Multisoft apparatus. Each experiment was performed three times.

2.9. Assessment of cell death using flow cytometry

Exponentially growing cells (2×10^6) were exposed to L-OHP, CPT-11 or combinations according to the previously described schedules. At each time point, floating cells were collected, adherent cells were trypsinised and pooled with the floating ones and suspensions were constantly kept at 4°. Trypsinisation procedure was first optimised by using trypan blue staining in order to ensure that living cells were not impaired by that process. A dual staining technique described by Ciancio *et al.* [26] was used to assess cell death in each sample. One million cells were washed in PBS before being suspended in 300 μL of a 20 μg/mL PI solution (Sigma) and kept on ice for 30 min. Cells were then permeabilised with 5.7 mL 25% ethanol in PBS and the suspension was homogenised. One hundred and fifty microliters of a 250 μM Hoechst 33342 (Sigma) solution were added, the suspension was vortex-mixed and stored at 4° for 48 hr to allow optimum staining before analysis.

Flow cytometric measurements were performed using a Beckman Coulter Epics ALTRA flow cytometer equipped with a Laser Enterprise II (Coherent) argon laser tuned to emit 60 mW in UV, a 450 nm band-pass filter for blue (Ho342) fluorescence and a 630 nm long-pass filter for red (PI) fluorescence. Ten thousand cells were analysed for each sample and quantitation was performed using Win MDI 2.8 software. Non-cellular material was excluded

from the analysis by gating right angle and forward angle light scattering characteristics of each population so that we could assume that cells with a DNA content inferior than 2*n* that appeared during the time course were apoptotic cells. Discrimination of viable, apoptotic and necrotic populations was performed by comparing dot plots to single-parameter (PI staining) frequency histograms and density plots. In the sorting procedure cells were sorted using an enrichment mode in tubes containing 0.5 mL foetal calf serum and their morphology was analysed after cytospin and haematoxylin–eosin staining.

2.10. Statistical analysis

Statistical analyses were performed using StatView 4.5 software (Abacus Concepts). All data are expressed as mean values ± SD from three independent experiments. The influence of tested schedules was analysed by means of ANOVA. A *post hoc* Fisher's protected least significant difference test was used to correct for multiple comparisons. A P value <0.05 was considered significant.

3. Results

3.1. Cytotoxic effects of the L-OHP/CPT-11 combination

In order to determine the optimal exposure to L-OHP, 1 and 24 hr-incubations were explored. The IC_{50} values were respectively 46.61 ± 1.32 and 1.23 ± 0.36 μM for HT29 cell line. The time-schedule dependency index [27] was high (37.9), which prompted us to use a 24-hr exposure. Fig. 1 and Table 1 respectively represent the dose–response curves of HT29 cells to L-OHP, CPT-11 and their combinations and the combination indices of the three tested schedules. A moderate synergism was observed when cells were exposed to the simultaneous combination ($CI_{50} = 0.72 \pm 0.04$) or to the CPT-11 → L-OHP sequence ($CI_{50} = 0.76 \pm 0.20$) whereas this effect was not observed when using the reverse combination ($CI_{50} = 1.09 \pm 0.31$).

Table 1
Combination indices (CI) for the *in vitro* interaction between oxaliplatin and irinotecan in HT29 cell line

Schedule	CI_{30}	CI_{50}	CI_{70}
L-OHP + CPT-11	0.89 ± 0.12	0.72 ± 0.04	0.59 ± 0.05
L-OHP → CPT-11	1.33 ± 0.52	1.09 ± 0.31	0.92 ± 0.15
CPT-11 → L-OHP	0.72 ± 0.23	0.76 ± 0.20	0.81 ± 0.15

CI_{30}, CI_{50}, CI_{70}: combination indices indicating the combined amount necessary to kill 30, 50 or 70%, respectively, of the cell population. Data are expressed as average values ± SD of three independent experiments.

3.2. Cell cycle phase distribution after exposure to L-OHP and/or CPT-11

In order to reveal potential differences in cell cycle progression, we assessed cell cycle phase distribution following the same treatments on adherent cells. While L-OHP treatment at IC_{50} transiently blocked cells in the G_2/M transition before cells accumulated in G_1 phase, 5 μM L-OHP resulted in a transient S phase delay followed with G_1 and G_2/M accumulation (Fig. 2A). When cells

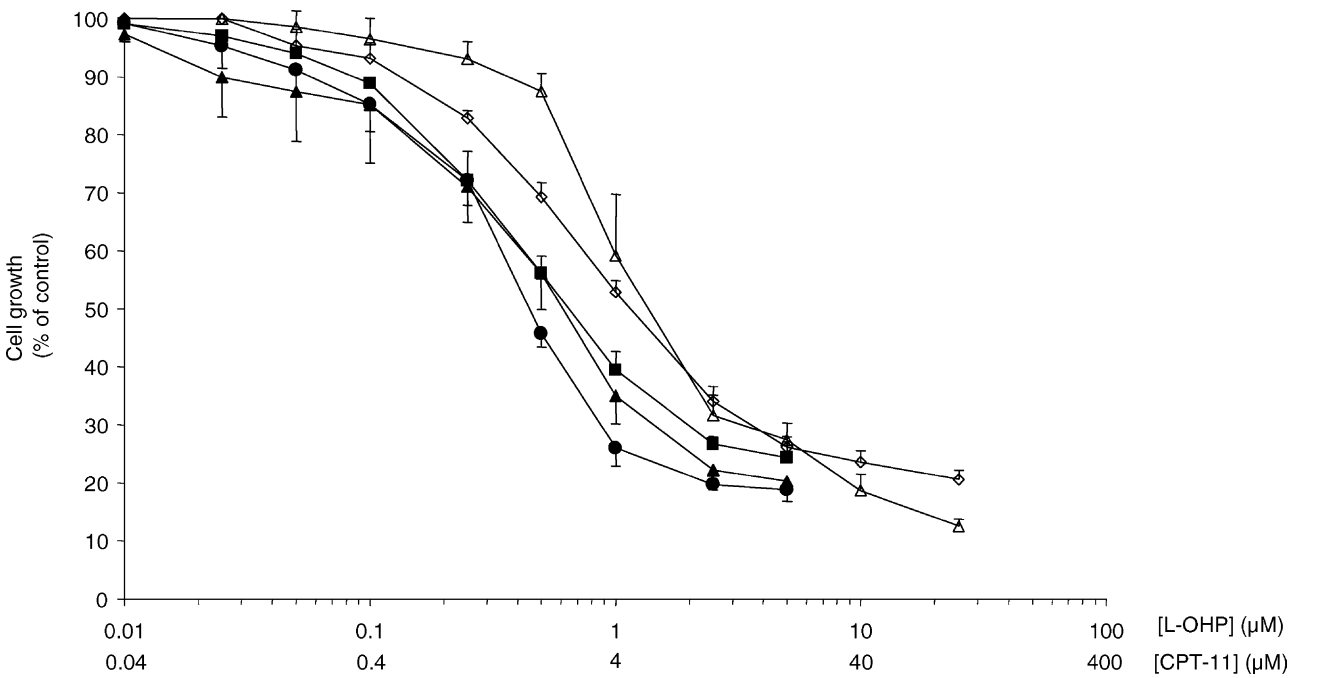

Fig. 1. Dose–response curves in HT29 colon adenocarcinoma cell line after exposure to CPT-11 (△), L-OHP (◇), L-OHP + CPT-11 (●), L-OHP → CPT-11 (■) and CPT-11 → L-OHP (▲). Cytotoxicity was evaluated using the sulforhodamine B technique. Data are expressed as mean values ± SD of three independent experiments.

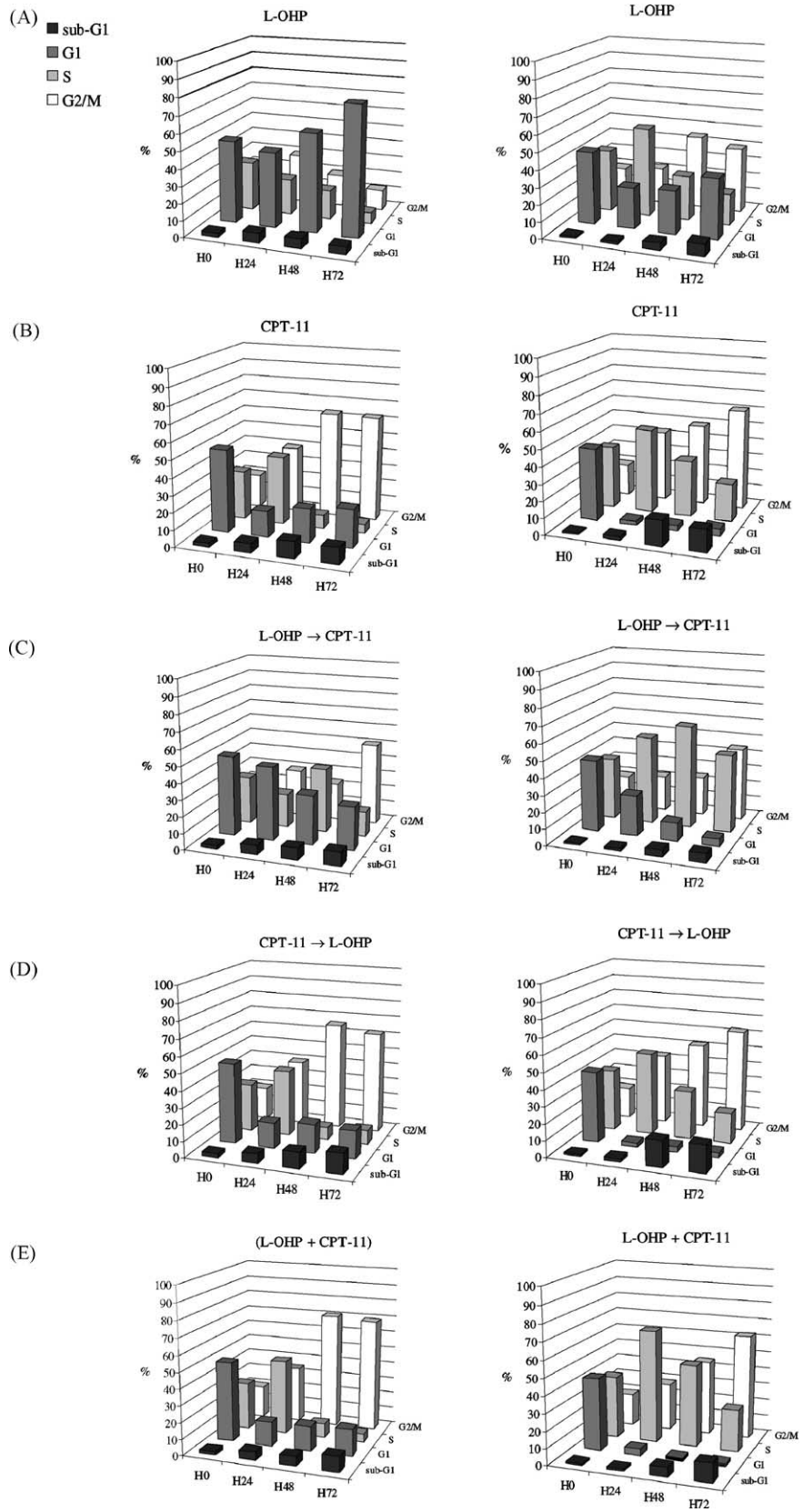

Fig. 2. Time course of cell cycle phase distribution after exposure to L-OHP (A), CPT-11 (B), L-OHP → CPT-11 (C), CPT-11 → L-OHP (D) and L-OHP + CPT-11 (E) combinations. Cells were exposed to 1.23 μM oxaliplatin and/or 4.6 μM irinotecan (left) or to 5 μM oxaliplatin and/or 20 μM irinotecan (right). Data are represented as mean values of three independent experiments.

were exposed to CPT-11 (Fig. 2B), a transient S phase block was observed at the end of the exposure and cells accumulated in the G_2/M phase. When cells were exposed to the L-OHP → CPT-11 sequence at the IC_{50} (Fig. 2C), a significant population remained in G_1 phase ($P < 0.05$) in relation to the other combinations while the population which was delayed in S phase accumulated in the G_2/M transition albeit in a lesser extent than with the two other combinations ($P < 0.0001$). Conversely, when cells were exposed to the CPT-11 → L-OHP sequence (Fig. 2D), S phase block was superior to the one observed when using CPT-11 alone (H72: $P = 0.0286$) while G_1 population was inferior to the one obtained using the Topo I inhibitor alone (H72: $P = 0.004$). With higher drug concentrations, the CPT-11 → L-OHP sequence generated a transient S phase accumulation followed with a constant increase in the G_2/M fraction. Exposure to the IC_{50} simultaneous combination (Fig. 2E) blocked cells in the G_2/M transition in a larger proportion than with CPT-11 alone (H48: $P = 0.0106$) without triggering the early appearance of a sub-G_1 fraction. At higher concentrations this exposure resulted in an important S phase delay (H48: $P = 0.0059$) and therefore late G_2/M accumulation and sub-G_1 fraction appearance.

3.3. Induction of DEVD–pNA cleaving activity and PARP cleavage by L-OHP and CPT-11

The time courses of PARP cleavage for the combination schedules as detected by Western blotting are shown in Fig. 3 and the results of DEVD–*p*NA cleaving activity are summarised in Table 2. When cells were exposed to the L-OHP → CPT-11 sequence, DEVDase activity and therefore PARP cleavage were late and moderate (Fig. 3D). Nevertheless, this combination and simultaneous exposure (Fig. 3C) induced a late but higher DEVD–*p*NA cleaving activity compared with L-OHP alone (H96: $P = 0.0021$ and 0.0003, respectively) when drugs were combined using IC_{50} concentrations. The CPT-11 → L-OHP sequence induced at IC_{50} substantial DEVD–*p*NA cleaving activity starting at the end of the exposure (H48: $P = 0.0008$) (Fig. 3E). This was confirmed using higher concentrations. Furthermore, at the end of the time course, this combina-

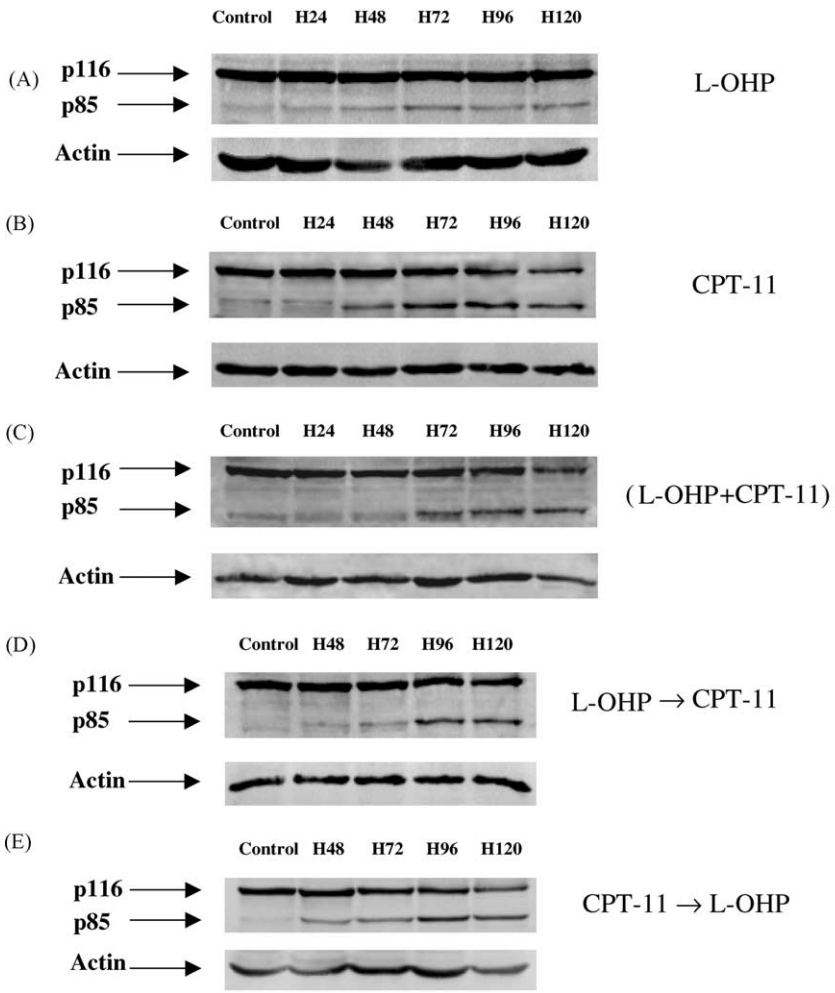

Fig. 3. Time course of PARP cleavage after exposure to 1.23 μM oxaliplatin (A), 4.6 μM irinotecan (B) or their combinations (C–E) as detected by Western blotting. Cells were exposed to L-OHP for 24 hr and/or CPT-11 for 24 hr whatever the combination. Data are representative of three independent experiments.

Table 2
Time course of DEVD–*p*NA cleaving activity in HT29 cell line after exposure to L-OHP/CPT-11 combinations

Schedule	DEVD–*p*NA cleaving activity (ΔDO/mg protein × 10^3)					
	H0	H24	H48	H72	H96	H120
Control	4 ± 2					
IC_{50}						
CPT-11		8 ± 1	18 ± 5	66 ± 15	109 ± 5	79 ± 3
L-OHP		7 ± 1	9 ± 2	18 ± 1	19 ± 6	18 ± 3
L-OHP + CPT-11		5 ± 3	15 ± 11	29 ± 7	53 ± 8*	65 ± 11*
L-OHP → CPT-11		7 ± 1	9 ± 1	16 ± 7	46 ± 5*	74 ± 2*
CPT-11 → L-OHP		8 ± 1	26 ± 2	48 ± 5	86 ± 13	114 ± 5**
IC_{70}						
CPT-11		19 ± 3	69 ± 23	154 ± 34	176 ± 14	193 ± 9
L-OHP		22 ± 8	27 ± 12	55 ± 26	105 ± 8	95 ± 16
L-OHP + CPT-11		25 ± 4	42 ± 11	80 ± 36	122 ± 35	101 ± 19
L-OHP → CPT-11			34 ± 8	46 ± 2	94 ± 14	105 ± 18
CPT-11 → L-OHP			102 ± 81	145 ± 109	126 ± 32	148 ± 52

Cells were exposed to 1.23 or 5 μM L-OHP and 4.6 or 20 μM CPT-11 for 24 hr whatever the combination. Data represent mean values ± SD of three independent experiments.

* $P < 0.05$, significantly different from oxaliplatin-treated cells as determined with Fisher's protected least significant difference test.

** $P < 0.05$, significantly different from irinotecan-treated cells as determined with Fisher's protected least significant difference test.

tion resulted in a DEVDase activity that was superior to the one induced by the other combinations and by CPT-11 alone (H120: $P < 0.0001$).

3.4. Identification of viable, apoptotic and necrotic populations by double-parameter flow cytometry

To further characterise the cytotoxic effect of the L-OHP/CPT-11 combinations, cells were exposed to the aforementioned schedules at concentrations superior than IC_{70} and cell death was assessed using a dual staining technique that allowed discriminating apoptotic from viable and necrotic populations. Viable cells, with undamaged plasma membranes, exclude PI and stain predominantly blue with Ho342 whereas necrotic cells, which cannot exclude PI, have more intense red fluorescence and proportionally lower blue fluorescence. The cells that undergo apoptosis show diminished Ho342 fluorescence and low PI fluorescence; at later stages they stain more with PI and less with Ho342. Double-staining analysis showed a moderate apoptotic phenomenon when cells were exposed to L-OHP alone (Fig. 4A) and revealed the early induction of substantial necrotic cell death starting 24 hr after the end of L-OHP exposure ($P < 0.05$). In contrast, apoptosis was the main biological effect triggered by CPT-11 (Fig. 4B). Kinetic profiles confirmed a delayed onset of apoptosis after exposure to the L-OHP → CPT-11 combination (Fig. 4D). The CPT-11 → L-OHP combination (Fig. 4E) generated an earlier apoptotic phenomenon and resulted in the induction of necrotic cell death which was superior to the one obtained with CPT-11 alone 24 hr after the end of the exposure ($P = 0.0068$) (Fig. 5). However, no significant difference was noted between the viable fractions of this combination and the single drug. Simultaneous exposure (Fig. 4C) generated an intermediate apoptotic response which was superior to the one induced by the L-OHP → CPT-11 combination and inferior to the CPT-11 → L-OHP sequence from H48 to the end of time course ($P < 0.05$). Moreover, the viable fraction was superior to the one observed with CPT-11 alone (H96: $P = 0.0374$). Cells were sorted upon their ability to exclude PI and analysed by microscopy after haematoxylin–eosin staining. One population mainly consisted of apoptotic bodies and cells with huge nuclei respect to controls. The second one, which did not exclude the permeant probe, was characterised by cell swelling with larger nucleoli and cytoplasms and frequently broken plasma membranes.

4. Discussion

Previous studies performed in our laboratory [28] evaluated the combination of CPT-11 with L-OHP in a panel of four human colon cell lines in order to assess whether synergism could be achieved whatever the used cell model. Synergism or additivity was observed in HCT-8, HCT-116 and HT29 cell lines while the combination was antagonistic in SW620 cells. This model-dependency prompted us to define the optimal schedule of exposure for a given cell line and identify cellular determinants involved in this interaction. Our preliminary work in the HT29 cell line showed that L-OHP cytotoxicity was time-dependent which led us to use a 24-hr exposure in combination with 24-hr CPT-11; the cytotoxicity of the latter is linked to the activity of a cytosolic carboxylesterase that produces the 1000-fold more potent Topo I inhibitor SN-38 [29] and to the duration of exposure necessary to convert most if not all the cleavable complexes into DNA double-strand breaks. The subsequent study demonstrated a sequence-dependent cytotoxicity for this combination. Synergism was observed

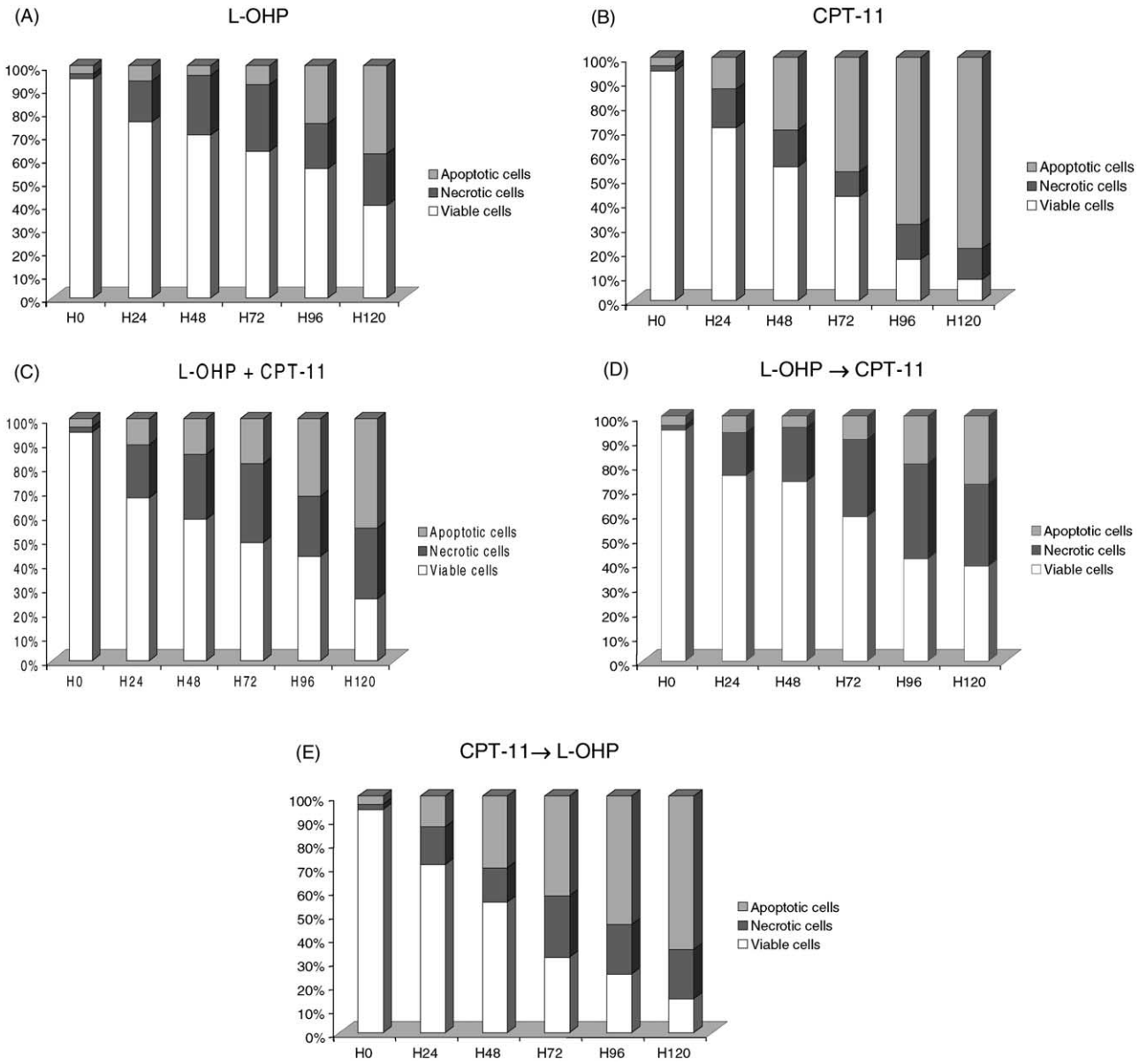

Fig. 4. Flow cytometric analysis of cell death time course in HT29 cells stained with Ho342 and propidium iodide. Cells were exposed to 5 μM L-OHP (A), 20 μM CPT-11 (B), L-OHP + CPT-11 (C), L-OHP → CPT-11 (D), or CPT-11 → L-OHP (E) combinations. Data are expressed as mean values of three independent experiments.

when cells were simultaneously exposed to drugs or first exposed to CPT-11 whereas the reverse sequential combination was rather additive. Our results are in accordance with previous reports describing positive interactions between a platinum compound and a Topo I inhibitor [30–35]. Nevertheless, one should keep in mind that besides the diversity of the cell models used in these studies, results have mostly been obtained after exposure to active chemical entities and not to prodrugs such as CPT-11, which might explain the moderate synergism we are reporting. Moreover, our work distinguishes from these studies by the 24-hr exposure to L-OHP which had rather been used as short (1–2 hr) or protracted (48–96 hr) exposures.

Our results led us to identify and characterise the origins of this cytotoxic effect. We first examined the distribution of viable cells in the different phases of the cell cycle. Cells exposed to CPT-11 alone were blocked in S phase before accumulating in the G_2/M transition. Camptothecin has been reported to induce an S phase accumulation characterised by DNA-PK activation and RPA2 phosphorylation. This phenomenon was abolished by exposure to the protein kinase inhibitor 7-hydroxystaurosporine, which suggested the existence of an S phase checkpoint mechanism [36]. The persistent depletion of the G_1 population when using high concentrations suggested that cells could not enter a new cycle and died by apoptosis. Ryan *et al.* [3] indeed reported that exposure to CPT-11 resulted in a

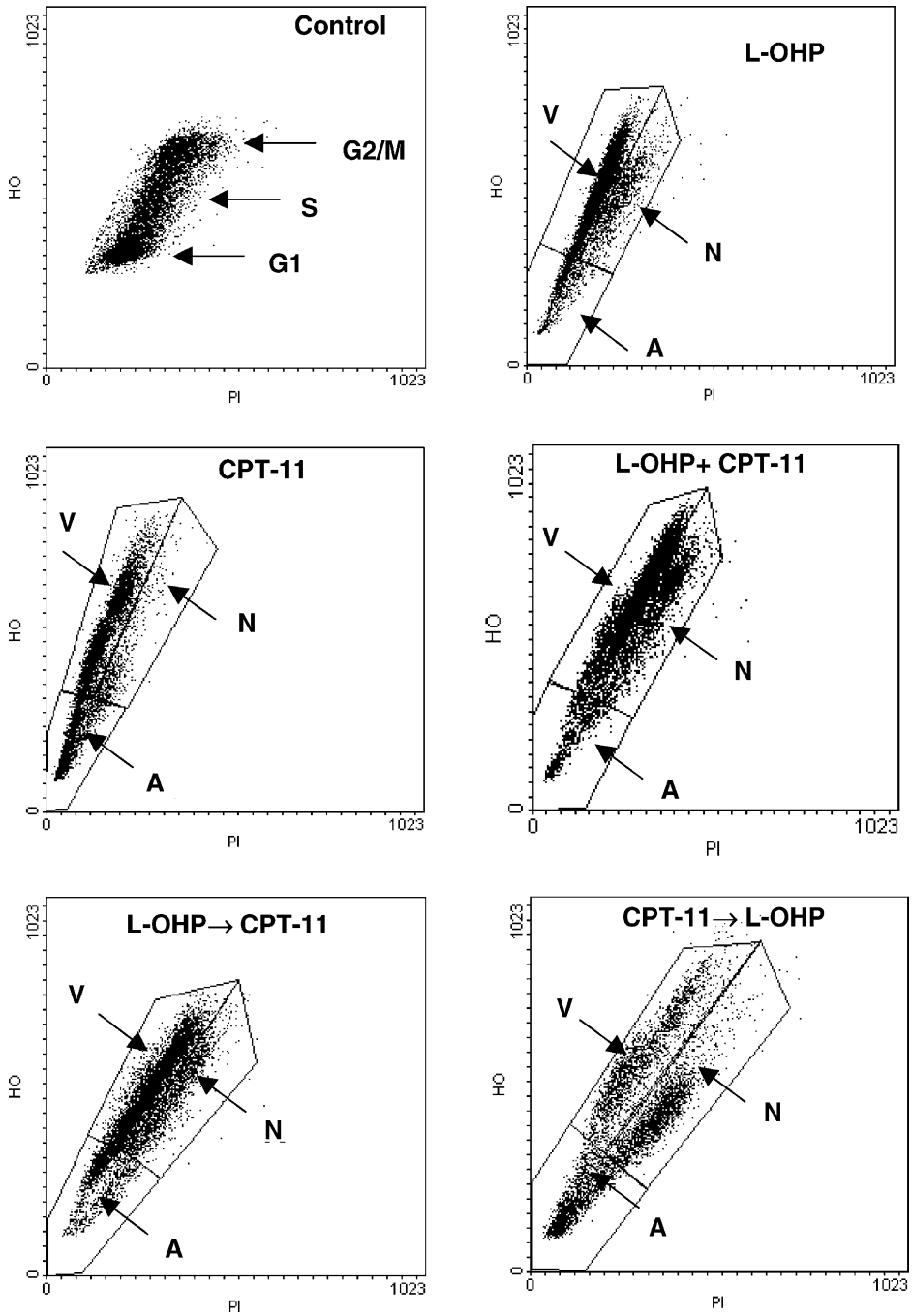

Fig. 5. Flow cytometric analysis of cell death performed at H72. Cells were exposed to 5 μM L-OHP, 20 μM CPT-11 or their combinations and stained with Ho342 and propidium iodide. Gating procedure representative of three independent experiments. V: viable, N: necrotic and A: apoptotic cells.

higher percentage of aberrant mitoses leading to cell death. On the other hand, cells exposed to L-OHP at IC_{50} were transiently blocked in the G_2/M transition before accumulating in the G_1 phase. However, when higher concentrations were used, cells accumulated in S phase but a significant population remained in G_1 phase at H24, suggesting that a fraction had been able to start another cell cycle due to repair [37] or translesion synthesis [38,39] past the lesions induced by the platinum compound. HT29 cell line exhibits a missense mutation on the p53 tumour suppressor gene [40] which abolishes its DNA-binding properties; the consequent loss of this sequence-specific transactivation activity prevents the synthesis of p21 and GADD45 necessary to G_1 arrest and repair and makes more crucial the G_2/M checkpoint which is therefore the only possibility to repair the lesions generated by cytotoxic drugs [41]. Nevertheless, further experiments might be helpful to explain how these cells were blocked in G_1 phase. Whatever the drug concentration, exposure to CPT-11 after L-OHP resulted in a persistent S phase delay and a lower G_2/M accumulation in relation to the other combinations. Topotecan and SN-38 have been reported to slow

down the reversal of L-OHP-induced DNA interstrand crosslinks in ovarian and colorectal cell lines, respectively [33,42]. Furthermore, the L-OHP → SN-38 combination increased the duration and extent of DNA and RNA synthesis inhibition induced by single drugs [42]. Since there are multiple pathways for regulating S phase at all stages further data is needed to explain the persistent S phase arrest in this L-OHP → CPT-11 combination. The cell cycle profile observed when using the CPT-11 → L-OHP sequence was in overall similar to the one induced by CPT-11 alone. However, the G_1 population was inferior when L-OHP was added after CPT-11 which suggests that this remaining fraction was affected by L-OHP. Exposure to the IC_{50} simultaneous combination resulted in the highest G_2/M accumulation without any significant increase in sub-G_1 fraction compared with the sequential combinations. At high concentrations this combination generated a significant S phase delay which was nonetheless inferior to the one observed in the L-OHP → CPT-11 sequence.

We then asked whether apoptosis was the main event in the observed synergism and focused our interest on cleavage of native enzyme PARP ($M_r \sim 116{,}000$) into an $M_r \sim 89{,}000$ catalytic domain and an $M_r \sim 25{,}000$ DNA-binding domain, which is a hallmark and an early phenomenon in programmed cell death [43,44]. The apoptotic signaling generated by L-OHP alone was late and moderate whereas CPT-11 induced a substantial PARP cleavage. The latter phenomenon paralleled the appearance of a significant sub-G_1 population. When cells were exposed to IC_{50} combinations DEVD–*p*NA cleaving activity triggered by the L-OHP → CPT-11 sequence or by the simultaneous combination were significantly higher than with L-OHP but lower than with CPT-11. This phenomenon paralleled the S phase perturbation which suggests that this L-OHP-induced S phase delay reduced the number of advancing replication forks, the collision of the latter with SN-38-induced cleavable complexes being a requisite for CPT-11 cytotoxicity. The CPT-11 → L-OHP sequence generated an earlier PARP cleavage with an earlier increase in DEVD–*p*NA cleaving activity. This phenomenon was emphasised using higher concentrations of both drugs. The cytotoxic gain in relation to CPT-11 alone was observed at the end of the time course where DEVDase activity was higher than the one triggered by CPT-11 alone. This might be due to the late effect of L-OHP on the remaining G_1 population after exposure to CPT-11. Finally, the concomitant exposure to these drugs resulted in an intermediate apoptotic response which could be due to the lower capacity of S phase-blocked cells to resume the cell cycle and accumulate in the G_2/M phase. This schedule might reveal a potential competition for Topo I activation or inhibition for respectively repair or trapping by SN-38. Another hypothesis might be a deeper S phase perturbation. Nevertheless, growth inhibition studies suggest that synergism observed in this combination can only be partly linked to its lethal and more precisely to its apoptotic effect. The most synergistic schedule did not indeed result in the highest apoptotic response.

We therefore asked whether apoptosis was the only cell death triggered by these combinations and performed double-parameter flow cytometry using PI and Ho342 staining. Simultaneous analysis of viable, necrotic and apoptotic populations exposed to concentrations higher than IC_{70} confirmed a drug-dependent feature of cell death. Apoptosis generated by the sequential combinations was conditioned by the first exposure. A significant apoptotic response was triggered in cells first exposed to CPT-11 whereas necrosis occurred in a larger proportion than programmed cell death when cells were first exposed to L-OHP. Exposure to the CPT-11 → L-OHP sequence resulted in a greater induction of necrosis compared with CPT-11 alone. This phenomenon might reflect cell failure to re-enter the cell cycle as a result of its inability to sustain acute damage although ATP-dependent repair processes have been mobilised. Besides ATP depletion can switch an ongoing apoptotic process into necrotic cell death, suggesting that intracellular ATP levels determine the mode of cell death [45,46]. Provided that viable populations were not different, the latter study suggests that L-OHP combined (or not) with CPT-11 might also have an impact on cell proliferation without inducing cell death. Of note, dot plots display a moderate shift in PI staining in necrotic respect to viable cells. In the general use of PI as a marker of necrotic cells, the red fluorescence increase is more obvious. However, previous studies have mostly been performed on haematological samples; therefore one cannot rule out the possibility that necrotic colon cell lines stain differently from these models. Besides exposure to L-OHP, CPT-11 or their combinations might also have unknown and different impacts on PI intercalation into double-strand nucleic acid.

The present work describes the sequence-dependent enhancement of the cytotoxicity of a third-generation platinum derivative by a Topo I inhibitor in a colon cancer cell line and confirms the relevance of such a combination in clinical practice. Identification of cellular determinants involved in this interaction and upstream receptor(s) triggering the apoptotic pathway is currently under investigation.

Acknowledgments

The authors wish to thank Fatima L'Faqihi-Olive for her technical assistance. S. Arnould received a grant from the Association pour la Recherche sur le Cancer.

References

[1] Pommier Y. Eukaryotic DNA topoisomerase I: genome gatekeeper and its intruders, camptothecins. Semin Oncol 1996;1(Suppl 3):3–10.
[2] Hsiang Y, Liu L. Identification of DNA topoisomerase I as an intacellular target of the anticancer drug camptothecin. Cancer Res 1988;48:1722–6.

[3] Ryan AJ, Squires S, Strutt HL, Evans A, Johnson RT. Different fates of camptothecin-induced replication fork-associated double-strand DNA breaks in mammalian cells. Carcinogenesis 1994;15:823–8.
[4] Shimada Y, Rothenberg M, Hilsenbeck SG, Burris III HA, Degen D, Von Hoff DD. Activity of CPT-11 (irinotecan hydrochloride), a topoisomerase I inhibitor, against human tumour colony-forming units. Anti-Cancer Drugs 1994;5(2):202–6.
[5] Kawato Y, Furuta T, Aonuma M, Yasuoka M, Yokokura T, Matsumoto K. Antitumour activity of a camptothecin derivative, CPT-11, against tumour xenografts in nude mice. Cancer Chemother Pharmacol 1991;28:192–8.
[6] Van Cutsem E, Cunningham D, Ten Bokkel Huinink W, Punt C, Alexopoulos C, Dirix L, Symann M, Blijham GH, Cholet P, Fillet G, Van Groeningen C, Vannetzel JM, Levi F, Panagos G, Unger C, Wils J, Cote C, Blanc C, Herait P, Bleiberg H. Clinical activity and benefit of irinotecan (CPT-11) in patients with colorectal cancer truly resistant to 5-fluorouracil (5-FU). Eur J Cancer 1999;35(1):54–9.
[7] Rougier P, Van Cutsem E, Bajetta E, Niederle N, Possinger K, Labianca R, Navarro M, Morant R, Bleiberg H, Wils J, Awad L, Herait P, Jacques C. Randomised trial of irinotecan versus fluorouracil by continuous infusion after fluorouracil failure in patients with metastatic colorectal cancer. Lancet 1998;352:1407–12.
[8] Ducreux M, Ychou M, Seitz JF, Bonnay M, Bexon A, Armand JP, Mahjoubi M, Mery-Mignard D, Rougier P. Irinotecan combined with bolus fluorouracil, continuous infusion fluorouracil, and high-dose leucovorin every two weeks (LV5FU2 regimen): a clinical dose-finding and pharmacokinetic study in patients with pretreated metastatic colorectal cancer. J Clin Oncol 1999;17(9):2901–8.
[9] Gil-Delgado MA, Antoine EC, Guinet F, Bassot V, Grapin JP, Benhammouda A, Adam R, Castaing D, Bismuth H, Khayat D. Phase I–II study of irinotecan in combination with mitomycin C in patients with advanced gastrointestinal cancer. Am J Clin Oncol 2001;24(3):251–4.
[10] Cvitkovic E, Wasserman E, Goldwasser F, Rougier P, Tigaud JM, Mahjoubi M, et al. Preliminary report on an oxaliplatin (L-OHP)/CPT-11 phase I trial in gastrointestinal (GI) malignancies: an active combination. Proc Am Soc Clin Oncol 1997;16:229a.
[11] Saris CP, van de Vaart PJM, Rietbroek RC, Blommaert FA. *In vitro* formation of DNA adducts by cisplatin, lobaplatin and oxaliplatin in calf thymus DNA in solution and in cultured human cells. Carcinogenesis 1996;17(12):2763–9.
[12] Raymond E, Lawrence R, Izbicka E, Faivre S, von Hoff DD. Activity of oxaliplatin against human tumour colony-forming units. Clin Cancer Res 1998;4:1021–9.
[13] Rixe O, Ortuzar W, Alvarez M, Parker R, Reed E, Paull K, Fojo T. Oxaliplatin, tetraplatin, cisplatin and carboplatin: spectrum of activity in drug-resistant cell lines and in the cell lines of the National Cancer Institute's anticancer drug screen panel. Biochem Pharmacol 1996;52(12):1855–65.
[14] Becouarn Y, Ychou M, Ducreux M, et al. Phase II trial of oxaliplatin as first-line chemotherapy in metastatic colorectal cancer patients. J Clin Oncol 1998;16(8):2739–44.
[15] de Gramont A, Vignoud J, Tournigand C, et al. Oxaliplatin with high-dose leucovorin and 5-fluorouracil 48-hr continuous infusion in pretreated metastatic colorectal cancer. Eur J Cancer 1997;33(2):214–9.
[16] Levi F, Misset JL, Brienza S, et al. A chronopharmacologic phase II clinical trial with 5-fluorouracil, folinic acid and oxaliplatin using an ambulatory multichannel programmable pump. Cancer 1992;69(4): 893–900.
[17] Wasserman E, Cuvier C, Lokiec F, Goldwasser F, et al. Combination of oxaliplatin plus irinotecan in patients with gastrointestinal tumours: results of two independent phase I studies with pharmacokinetics. J Clin Oncol 1999;17(6):1751–9.
[18] Scheithauer W, Kornek GV, Raderer M, et al. Combined irinotecan and oxaliplatin plus granulocyte colony-stimulating factor in patients with advanced fluoropyrimidine/leucovorin-pretreated colorectal cancer. J Clin Oncol 1999;17(3):902–6.
[19] Jacobson MD, Weil M, Raff MC. Programmed cell death in animal development. Cell 1997;88:347–54.
[20] Schulze-Osthoff K, Ferrari D, Los M, Wesselborg S, Peter ME. Apoptosis signaling by death receptors. Eur J Biochem 1998;254:439–59.
[21] Kaufmann SH. Induction of endonucleolytic DNA cleavage in human acute myelogenous leukemia cells by etoposide, camptothecin and other cytotoxic anticancer drugs: a cautionary note. Cancer Res 1989;49(21):5870–8.
[22] Skehan P, Storeng R, Scudiero D, Monks A, McMahon J, Vistica D, Warren JT, Bokesch H, Kenney S, Boyd MR. New colorimetric cytotoxicity assay for anticancer-drug screening. J Natl Cancer Inst 1990;82(13):1107–12.
[23] Chou TC, Talalay P. Quantitative analysis of dose–effect relationships: the combined effects of multiple drugs or enzyme inhibitors. Adv Enzyme Regul 1984;22:27–55.
[24] Bradford MM. A rapid and sensitive method for the quantitation of microgram quantities of protein utilising the principle of protein–dye binding. Anal Biochem 1976;72:248–54.
[25] He J, Whitacre CM, Xue LY, Berger NA, Oleinick NL. Protease activation and cleavage of poly(ADP-ribose) polymerase: an integral part of apoptosis in response to photodynamic treatment. Cancer Res 1998;58:940–6.
[26] Ciancio G, Pollack A, Taupier MA, Block NL, Irvin III GL. Measurement of cell-cycle phase-specific cell death using Hoechst 33342 and propidium iodide: preservation by ethanol fixation. J Histochem Cytochem 1988;36(9):1147–52.
[27] Matsushima Y, Kanzawa F, Hoshi A, Shimizu E, Nomori H, Sasaki Y, Saijo N. Time-schedule dependency of the inhibiting activity of various anticancer drugs in the clonogenic assay. Cancer Chemother Pharmacol 1985;14(2):104–7.
[28] Guichard S, Arnould S, Hennebelle I, Bugat R, Canal P. Combination of oxaliplatin and irinotecan on human colon cancer cell lines: activity *in vitro* and *in vivo*. Anti-Cancer Drugs 2001;12(9):741–51.
[29] Kawato Y, Aonuma M, Hirota Y, Kuga H, Sato K. Intracellular roles of SN-38, a metabolite of the camptothecin derivative CPT-11, in the antitumour effect of CPT-11. Cancer Res 1991;51(16):4187–91.
[30] Goldwasser F, Valenti M, Torres R, Kohn KW, Pommier Y. Potentiation of cisplatin cytotoxicity by 9-aminocamptothecin. Clin Cancer Res 1996;2:687–93.
[31] Kano Y, Suzuki K, Akutsu M, Suda K, Inoue Y, Yoshida M, Sakamoto S, Miura Y. Effects of CPT-11 in combination with other anti-cancer agents in culture. Int J Cancer 1992;50(4):604–10.
[32] Chou TC, Motzer RJ, Tong Y, Bosl GJ. Computerised quantitation of synergism and antagonism of taxol, topotecan, and cisplatin against human teratocarcinoma cell growth: a rational approach to clinical protocol design. J Natl Cancer Inst 1994;86(20):1517–24.
[33] Goldwasser F, Bozec L, Zeghari-Squalli N, Misset JL. Cellular pharmacology of the combination of oxaliplatin with topotecan in the IGROV-1 human ovarian cancer cell line. Anti-Cancer Drugs 1999;10(2):195–201.
[34] Ma J, Maliepaard M, Nooter K, Boersma AW, Verweij J, Stoter G, Schellens JH. Synergistic cytotoxicity of cisplatin and topotecan or SN-38 in a panel of eight solid-tumour cell lines *in vitro*. Cancer Chemother Pharmacol 1998;41(4):307–16.
[35] Fischel JL, Rostagno P, Formento P, Dubreuil A, Etienne MC, Milano G. Ternary combination of irinotecan, fluorouracil–folinic acid and oxaliplatin: results on human colon cancer cell lines. Br J Cancer 2001;84(4):579–85.
[36] Shao RG, Cao CX, Zhang H, Kohn KW, Wold MS, Pommier Y. Replication-mediated DNA damage by camptothecin induces phosphorylation of RPA by DNA-dependent protein kinase and dissociates RPA:DNA-PK complexes. EMBO J 1999;18(5):1397–406.
[37] Reardon JT, Vaisman A, Chaney SG, Sancar A. Efficient nucleotide excision repair of cisplatin, oxaliplatin, and bis-aceto-ammine-dichloro-cyclohexylamine-platinum(IV) (JM216) platinum intrastrand DNA diadducts. Cancer Res 1999;59(16):3968–71.

[38] Vaisman A, Masutani C, Hanaoka F, Chaney SG. Efficient translesion replication past oxaliplatin and cisplatin GpG adducts by human DNA polymerase eta. Biochemistry 2000;39(16):4575–80.
[39] Vaisman A, Chaney SG. The efficiency and fidelity of translesion synthesis past cisplatin and oxaliplatin GpG adducts by human DNA polymerase beta. J Biol Chem 2000;275(17):13017–25.
[40] Rodrigues NR, Rowan A, Smith ME, Kerr IB, Bodmer WF, Gannon JV, Lane DP. p53 mutations in colorectal cancer. Proc Natl Acad Sci USA 1990;87(19):7555–9.
[41] Goldwasser F, Shimizu T, Jackman J, Hoki Y, O'Connor PM, Kohn KW, Pommier Y. Correlations between S and G2 arrest and the cytotoxicity of camptothecin in human colon carcinoma cells. Cancer Res 1996;56(19):4430–7.
[42] Zeghari-Squalli N, Raymond E, Cvitkovic E, Goldwasser F. Cellular pharmacology of the combination of DNA topoisomerase I inhibitor SN-38 and the diaminocyclohexane platinum derivative oxaliplatin. Clin Cancer Res 1999;5(5):1189–96.
[43] Lazebnik YA, Kaufmann SH, Desnoyers S, Poirier GG, Earnshaw WC. Cleavage of poly(ADP-ribose) polymerase by a proteinase with properties like ICE. Nature 1994;371(6495):346–7.
[44] Kaufmann SH, Desnoyers S, Ottaviano Y, Davidson NE, Poirier G. Specific proteolytic cleavage of poly(ADP-ribose) polymerase: an early marker of chemotherapy-induced apoptosis. Cancer Res 1993;53:3976–85.
[45] Eguchi Y, Shimizu S, Tsujimoto Y. Intracellular ATP levels determine cell death fate by apoptosis or necrosis. Cancer Res 1997;57:1835–40.
[46] Leist M, Single B, Castoldi AF, Kühnle S, Nicotera P. Intracellular adenosine triphosphate (ATP) concentration: a switch in the decision between apoptosis and necrosis. J Exp Med 1997;185(8): 1481–6.